Available online at www.sciencedirect.com

ScienceDirect

Progress in Natural Science: Materials International 24 (2014) 121–127

Progress in Natural Science Materials International

www.elsevier.com/locate/pnsmi
www.sciencedirect.com

Original Research

Investigation of the microcrack evolution in a Ti-based bulk metallic glass matrix composite

Yongsheng Wang[a], Zhenxi Guo[b], Rui Ma[a], Guojian Hao[a,*], Yong Zhang[a], Junpin Lin[a], Manling Sui[b]

[a]*State Key Laboratory for Advanced Metals and Materials, University of Science and Technology Beijing, Beijing 100083, China*
[b]*Institute of Microstructure and Property of Advanced Materials, Beijing University of Technology, Beijing 100124, China*

Received 28 August 2013; accepted 20 December 2013
Available online 9 May 2014

Abstract

The initiation and evolution behavior of the shear-bands and microcracks in a Ti-based metallic-glass–matrix composite (MGMC) were investigated by using an *in-situ* tensile test under transmission electron microscopy (TEM). It was found that the plastic deformation of the Ti-based MGMC related with the generation of the plastic deformation zone in crystalline and shear deformation zone in glass phase near the crack tip. The dendrites can suppress the propagation of the shear band effectively. Before the rapid propagation of cracks, the extending of plastic deformation zone and shear deformation zone ahead of crack tip is the main pattern in the composite.

Keywords: Metallic glass; Composites; Transmission electron microscopy; Ti alloys; Mechanical properties

1. Introduction

Recently, bulk metallic glasses (BMGs) have attracted considerable interest due to the distinguished mechanical properties, e.g. extraordinary strengths, high hardness and elastic yield strains [1–5]. However, the monolithic BMGs at room temperature exhibit a poor macroscopic plasticity for the highly localized shear deformation, which has severely hindered their engineering applications [3–11]. The improvement of the macroplasticity in BMGs continues to be an exciting area for material science. Metallic-glass–matrix (MGM) composites with *in-situ* dendrites reinforced, as an effective approach for improving the plasticity and toughness, have received wide attention such as Ti- [2,6], Zr- [3,5,7,8], Mg- [9], La- [10] and Cu-based [11] MGM composites, *etc.* Compared with monolithic BMGs and their crystalline counterparts, these composites share the advantages of large plastic deformation and high strength by the combination of dendrites and the glass phase [5–11]. And the studies of deformation mechanism have demonstrated that the large plastic deformation and the toughness result from prohibiting the unconstrained propagation of the individual shear-band, and initiating profuse shear-bands by dendrites. Moreover, dislocations, slipping and martensitic transformation *etc.* in dendrites have a significant contribution to the plasticity of MGM composites [2,3,5–11].

However, the macroscopic fractography does not provide the insights on the microscopic correlation between propagation of shear-band in glass phase as well as plastic deformation in dendrites and the crack extension of MGM composites. The *in-situ* tensile test under transmission electron microscopy (TEM) should be a suitable and powerful tool for the direct observation of deformation behavior at nanometer scale, *e.g.* observing the microcrack propagation and blunting [12], the emission and motion of the dislocations at the tip of the crack

*Corresponding author. Tel.: +86 10 62332192; fax: +86 10 82375390.
E-mail address: drhaogj@gmail.com (G. Hao).
Peer review under responsibility of Chinese Materials Research Society.

Production and hosting by Elsevier

http://dx.doi.org/10.1016/j.pnsc.2014.03.010
1002-0071/

in crystal alloys [13]. Previous studies on the monolithic BMGs showed that the jump-like shear-bands propagation process was observed, the secondary shear-bands were correlated with the jump sites [14]. The nanoparticles were formed in the shear-band tip, which can effectively blunt cracks [15]. Pekarskaya et al. [16] reported that the shear-bands path in the Zr-based MGM composite was not along a steady 'plane', and observed a large number of shear-bands in the glass matrix and the localization of deformation in the dendrite. However, the investigation using *in-situ* TEM in a BMG containing nanoparticles showed that the nanocrystals grow in shear-bands, which connected with shear delocalization and crack blunting [17]. Though some significant progress has been made, problems in the initiation of shear-bands, especially, the process of propagation and the evolution between the glass matrix and then dendrites remains few reports.

In this paper, detailed observations of the initiation, propagation and evolution of microcracks in a Ti-based MGM composite were investigated by using an *in-situ* tensile test under TEM.

2. Experimental

The master alloy with a nominal composition of $Ti_{47}Zr_{19}Be_{15}V_{12}Cu_7$ (at%) was prepared by arc-melting the mixture of high purity elements (purity $>99.9\%$) under argon atmosphere. A composite sample was fabricated by Bridgman solidification [18]. Foils from the current composite were thinned by the ion milling under liquid nitrogen temperature to produce a central hole, and subsequently mounted on a tensile straining device for *in-situ* deformation in a Gatan model 654 single-tilt straining holder and a FEI Tecnai F30 TEM operating at 300 kV.

Fig. 1 shows the picture of the *in-situ* TEM tensile holder (a), and the Cu-plate for holding a TEM sample (b). *In-situ* TEM observations were performed at the rate of 1 μm/s, and interrupted several times to observe changes of the microstructure and evolution of plastic deformation during the different periods of tensile straining at room temperature. More details can be seen in the references of [19–21]. The instrumental nanoindentation experiment was performed by Nano indenter II with Berkovich pressure head and repeated at least 5 times to ensure the reliability.

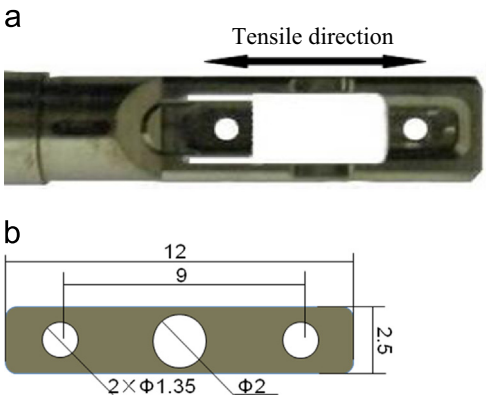

Fig. 1. The picture of an *in-situ* TEM tensile holder (a), and the Cu-plate for holding a TEM sample (b).

3. Results

3.1. Formation of the shear-band and the microcrack

Fig. 2 shows a typical bright-field TEM image of a current composite sample prior to tensile deformation. The composite consists of the dendrite phase with dimension of 2–15 μm and the amorphous matrix. The body-centered cubic (B.C.C.) structure of the dendrite with lattice parameter of 0.3201 nm and the glass phase with homogeneous maze can be identified by selected area electron diffraction (SAED) pattern.

Fig. 3 illustrates the generating of a microcrack in the current composite. Compared with Fig. 3(a), the band-like thin plastic deformation zone (PDZ) with thickness of 100 nm and length about 1 μm, as marked "An" in Fig. 3(b), formed ahead of the microcrack tip in dendrites, but was prohibited by the interface. According to the theoretical analysis and previous results [4,21–27], the band-like thinned deformation zone ahead of the microcrack tip without generating new surface can be considered as the shear deformation zone (SDZ) in glass matrix where shear-bands were formed, and the PDZ in dendrite phase. Although the initiated direction of the microcrack is perpendicular to the loading direction, but the propagated direction changed slightly in dendrite (point "A"), as shown in Fig. 3(c). Clearly, the dark striations in the images are bend contours, but it only can be observed in the dendrite phase. Similar phenomenon also can be observed in the TEM images of MGM composites [3,6,16,28–30].

Fig. 4 shows the initiation of shear deformation in the amorphous phase. Fig. 4(a) and (b) shows a central hole prior to deformation and its SAED pattern. The shear-band "mn" with thickness about 50 nm as well as length scale of 500 nm formed along the direction of maximal shear stress (about 45°), as illustrated in Fig. 4(c). It should be noted that the SDZ is also a common deformation characteristic in the glass matrix like the PDZ in dendrites. After fracture, the fracture surface displays that shear-bands over several hundred nanometers to a few micrometers is restricted to a zone with numerous shear planes stacked on the top of each other instead of an individual shear plane by the image contrast, as shown in Fig. 4(d). It is consistent with the previous report [16]. For monolithic BMGs, the feature was considered as "liquid-like layer" for local intense heating which even bring out nanocrystallization [14,15].

3.2. Evolution characteristics of the deformation zone

Fig. 5 demonstrates the evolution of a preexisting microcrack in a single dendrite. The artificial crack with a PDZ "mn" can be observed in Fig. 5(a). With increasing of the applied stress, the crystalline would become thinner and thinner because of dislocation multiplication and motion [13,16]. The microcrack tip (marked by "m") extended along the PDZ where many finer branches formed with the further

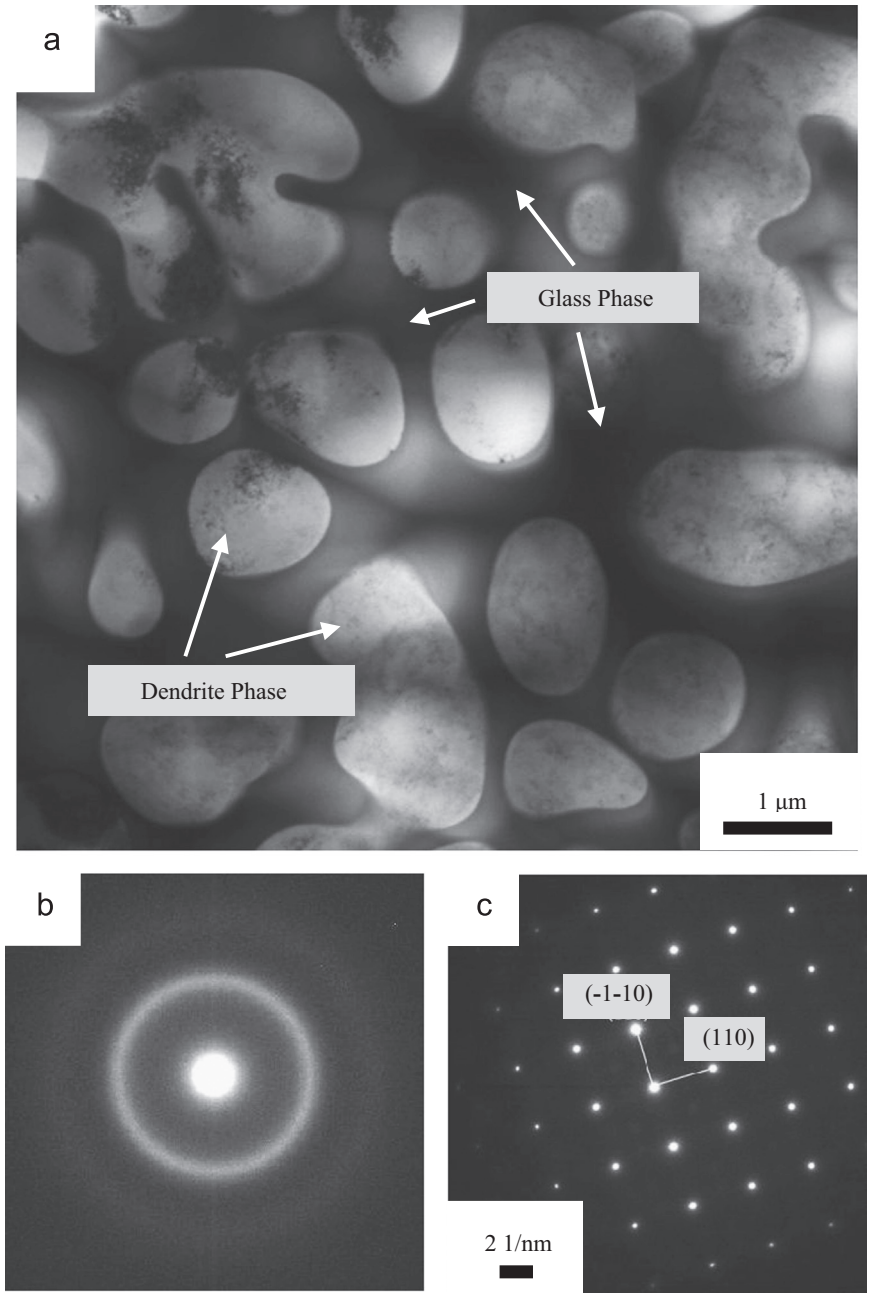

Fig. 2. A TEM image of a Ti-based MGM composite at low magnification in (a), and the SAED pattern of the amorphous phase (b) and the dendrite phase (c).

loading. By carefully comparison of Fig. 5(a)–(c), we found that the microcrack had slightly propagated along the PDZ. The plastic transition area connects the crack tip and elastic zone, as a guide to promote the ductile of the composite.

3.3. The change of the extending direction

Fig. 6 demonstrates deflection of the extending direction. Apparently, the extension direction of a microcrack from the amorphous phase to the dendrite diverged to the dendrite-side (along "mn" in Fig. 6(a)), and left a nanovoids along the initial direction. However, the extending direction changed again, slide along the interface instead of the propagation along "mn". Fig. 6(b) shows the microcrack propagated along plastic zone (length scale ~3 μm) involve the PDZ and SDZ, "mn", and the extension direction slightly deviated the original crack direction. Generally, it is hard to observe the propagation of shear-band during loading, because the formation and propagation of the major shear-band in monolithic BMGs occur simultaneously under tensile loading.

4. Discussion

For monolithic BMGs [31–33], prior work has documented that the competition between the creation and annihilation of free volume determines the final mechanical properties.

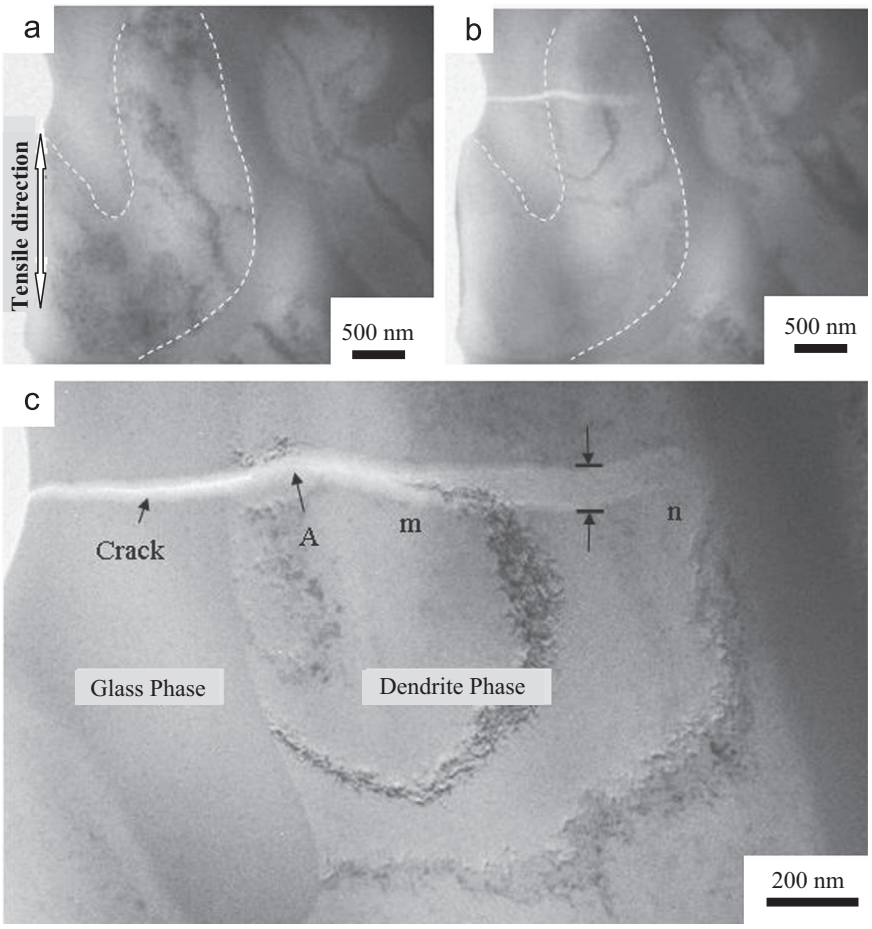

Fig. 3. TEM images of the initiation of the shear-band and the microcrack. (a) The thin specimen by an ion milling before loading, (b) the deformed specimen and it is the enlarge image in (c).

If annihilation rate of free volume surpassed the concentration rate, the stable plastic deformation and strain hardening generated [33], but when the total concentration of free volumes increased for the concentration rate beyond the annihilation rate, shear-bands formed by generating new surfaces [31,32]. However, for *in-situ* MGM composites, the ordered crystalline phase and the disordered amorphous phase have different physical and mechanical properties. From Table 1, the dendrite phase has the lower modulus and strength than the amorphous phase. Upon tensile loading, when the loading stress satisfies the yielding stress of dendrites, dendrites yield firstly by initiating the dislocation glide [34,35]. It agrees with the previous results [3,6] and *in-situ* observation [16].

However, in this study we found a crack originated from the amorphous matrix along the normal stress direction, as shown in Fig. 3. Here, the normal stress, σ_α, and the shear stress, τ_α, can be expressed as follows [36]:

$$\sigma_\alpha = \sigma \cos 2\alpha$$
$$\tau_\alpha = \sigma \sin 2\alpha, \quad (1)$$

where σ is the tensile stress, α is the initiation direction of shear-bands. From Eq. (1), when α is 90°, the σ_α attains the maximum value, $\sigma_\alpha = \sigma$, but the τ_α, does not exist, $\tau_\alpha = 0$. The normal stress promotes voids to form shear-bands [37]. During the further loading, the stress peak in any imperfections could reach the cohesive strength of atoms in these composites, resulting in an irreversible SDZ/PDZ. In addition, a microcrack would generate nearby the center hole for the inhomogeneous thickness.

Once the dendrite yielded, dislocations formed and multiplied. But the interface and amorphous phase prohibited the motion of dislocations, resulting in the higher stress nearby the interface. The crack propagation of materials is analyzed by Irwin's model which focuses on the propagation along the crack axis [38]. Under plane stress conditions, the relation of applied stress, σ, to the stress intensity factor K_I is

$$\sigma = K_I/\sqrt{2\pi x}, \quad (2)$$

When the applied stress increased largely enough to reach or exceed the atomic cohesive strength, the equilibrium of stress field nearby the tip would be destroyed. The original microcrack should spread by a length R to fulfill the stress equilibrium of the crack tip [39,40]. The distance R is SDZ in amorphous matrix or PDZ in dendrites from the crack tip to the interface between plastic and elastic zone. The narrow SDZ with a lower density have a lower strength, because of the presence of atomic clusters and free volume [31–33]. The extension of microcracks is preferentially by local atomic clusters instead of atoms. The propagation length scale of shear-bands is 0.1–1 μm for Zr-based

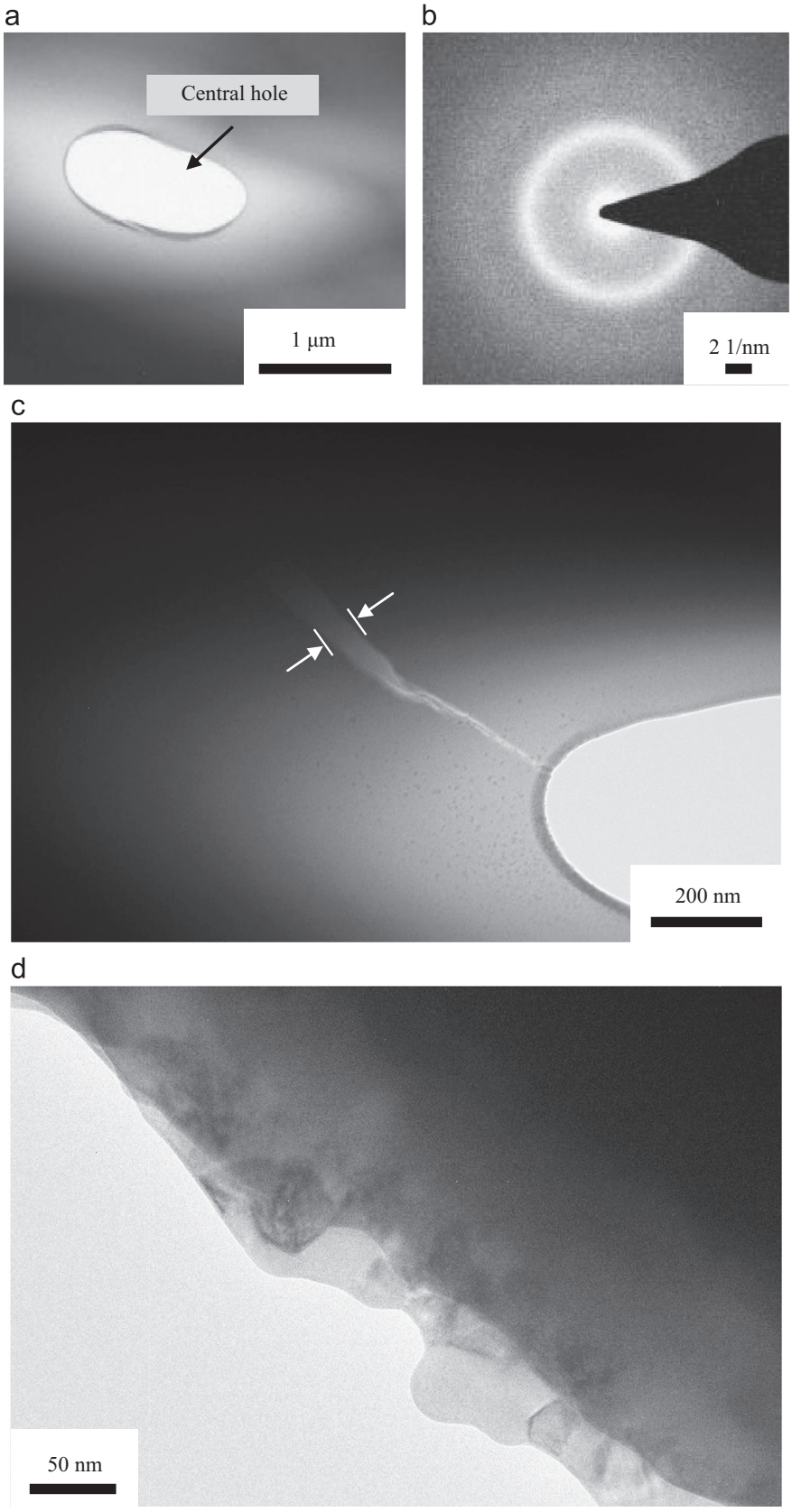

Fig. 4. TEM images of the initiation of shear deformation in the amorphous phase. (a) A centre hole prior to deformation, and its SAED pattern (b), (c) a shear-band formed after further loading and (d) the fracture surface.

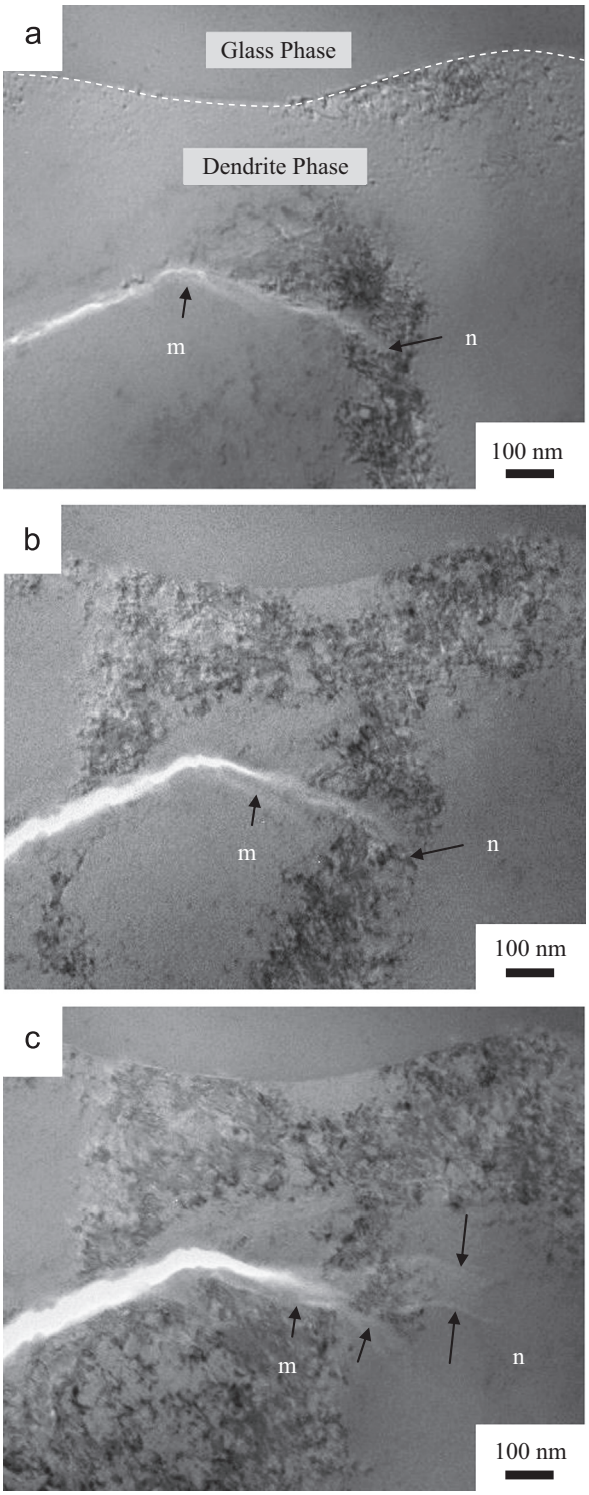

Fig. 5. Crack propagating in the dendrite (a), a preexisting microcrack image (b) and (c) the images after the first and further loading.

BMGs, which is consistent with the above observations in Figs. 3 and 6.

A great many of experimental results such as the compression [1,4], tension [2,3,41], and fatigue tests [7,8] *etc.* in the *in-situ* MGM composites indicate that the deflection of shear-bands propagation plays a positive role for the improvement of

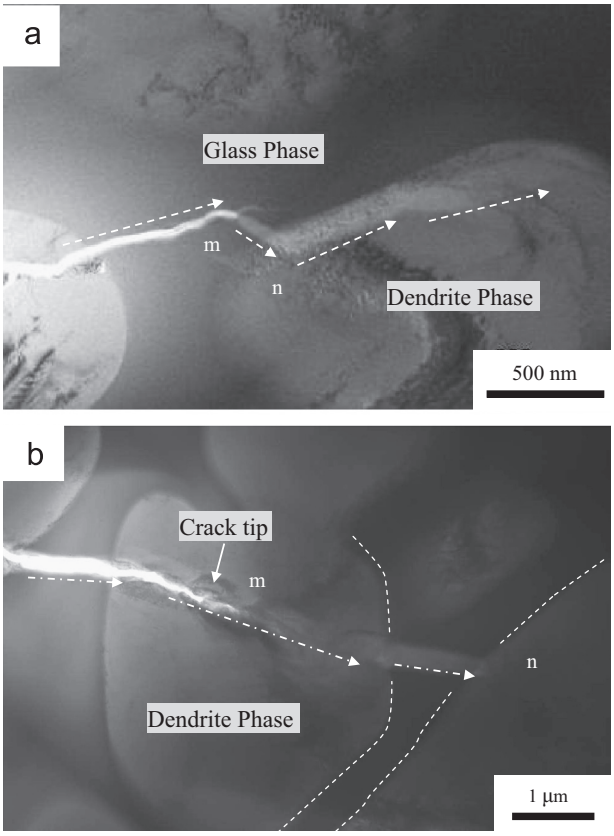

Fig. 6. The observation of the crack deflection and propagation between the two phases: (a) from the amorphous phase to the dendrite phase, and (b) from the dendrite phase to the amorphous phase.

Table 1
The Modulus (M), Hardness (H) and Yield stress (σ) of the dendrite phase and amorphous phase, $H \approx 3\sigma$.

	M (MPa)	H (GPa)	σ (MPa)
dendrite	105	4.786	1519
matrix	114	6.614	2205

the plasticity. Fig. 6(a) shows that a microcrack with an oblique angle of extension direction deflected along the interface. However, Figs. 3(c) and 6(b) demonstrate that the microcrack penetrated the amorphous phase into the dendrite with slightly deflection of extension direction, and initiated the PDZ at the tip of the crack. Here, we assume that shear-bands propagated under the shear stress, τ_α, along the α_i direction, the shear strain,ε, can be expressed as [34]:

$$\varepsilon = \sum_{i=1}^{N} \varepsilon_1^p = \sum_{i=1}^{N} \frac{\gamma_i \cos \alpha_i \sin \alpha_i}{\kappa} = \sum_{i=1}^{N} \frac{\gamma_i \sin 2\alpha_i}{2\kappa}, \quad (3)$$

where γ_i is the contribution of shear-bands propagation to the global plastic tensile strain, ε_1^p. N is the number of propagated shear-bands under tensile loading, and k is the ratio of the length to width in the gauge portion. When a microcrack propagated from the amorphous phase to the dendrite phase, the fracture mode changed from the brittle pattern to the ductile one. As a result, the stress balance near the crack tip is destroyed. From Eqs. (1) and (3), when the propagation direction is along 45°,

not only the shear stress can attain the maximum value, $\tau_\alpha=\sigma$, but also the ε has the largest value. The crack to perpendiculars to perpetrate the interface is resulted from the stress state of pure mode I at the crack tip, however, the deflection of the microctack corresponds to a mixed mode [40]. Therefore, although two patterns of propagation direction of the microcrack can be roughly observed from Figs. 3 and 6, the deflection of the extending direction prone to trigger along the maximum shear stress. Anyway, either the growth of length or the deflection of the microcrack is to release the excess energy to keep the energy balance nearby the crack tip.

5. Conclusion

In this study, the generation and propagation of the microcrack in a Ti-based MGM composite has been investigated by an *in-situ* TEM tensile test. Dendrites with the remarkable plastic deformation ability can accommodate the propagation of a microcrack. The nanoscopic crack propagates though a PDZ in dendrites and SDZ in amorphous phase. The change of the extending direction relates with the maximum shear stress and shear strain.

Acknowledgments

The authors would like to acknowledge the financial support of the National Natural Science Foundation of China (Grant no. 51001008) and the Fundamental Research Funds for the Central Universities (FRF-MP-10-005B).

References

[1] C.C. Hays, C.P. Kim, W.L. Johnson, Phys. Rev. Lett. 84 (2000) 2901–2904.
[2] D.C. Hofmann, J.Y. Suh, A. Wiest, M.L. Lind, M.D. Demetriou, W.L. Johnson, Proc. Natl. Acad. Sci. USA 105 (2008) 20136–20140.
[3] D.C. Hofmann, J.Y. Suh, A. Wiest, G. Duan, M.L. Lind, M.D. Demetriou, W.L. Johnson, Nature 451 (2008) 1085–1090.
[4] Y.H. Liu, C.T. Liu, A. Gali, A. Inoue, M.W. Chen, Intermetallics 18 (2010) 1455–1464.
[5] J.W. Qiao, E.W. Huang, F. Jiang, T. Ungár, G. Csiszár, L. Li, Y. Ren, P.K. Liaw, Y. Zhang, Appl. Phys. Lett. 97 (2010) 171910–171913.
[6] J.W. Qiao, A.C. Sun, E.W. Huang, Y. Zhang, P.K. Liaw, C.P. Chuang, Acta Mater. 59 (2011) 4126–4137.
[7] G.Y. Wang, P.K. Liaw, W.H. Peter, B. Yang, M. Freels, Y. Yokoyama, M.L. Benson, B.A. Green, T.A. Saleh, R.L. McDaniels, R.V. Steward, R.A. Buchanan, C.T. Liu, C.R. Brooks, Intermetallics 12 (2004) 1219–1227.
[8] G.Y. Wang, P.K. Liaw, A. Peker, B. Yang, M.L. Benson, W. Yuan, W.H. Peter, L. Huang, M. Freels, R.A. Buchanan, C.T. Liu, C.R. Brooks, Intermetallics 13 (2005) 429–435.
[9] X. Hui, W. Dong, G.L. Chen, K.F. Yao, Acta Mater. 55 (2007) 907–920.
[10] Y. Zhang, M.L. Lee, H. Tan, Q. Jing, Y. Li, Intermetallics 12 (2004) 1279–1283.
[11] Y. Wu, Y. Xiao, G. Chen, C.T. Liu, Z. Lu, Adv Mater. 22 (2010) 2733–2770.
[12] M. Legros, D.S. Gianola, K.J. Hemker, Acta Mater. 56 (2008) 3380–3393.
[13] H. Lu, Y. Su, Y. Wang, W. Chu, Corro. Sci. 41 (1999) 699–708.
[14] D.T.A. Matthews, V. Ocelík, P.M. Bronsveld, J.T.M. De Hosson., Acta Mater. 56 (2008) 1762–1773.
[15] G. Wilde, H. Rösner., Appl. Phys. Lett. 98 (2011) 251904–251907.
[16] E. Pekarskaya, C.P. Kim, A.W.L. Johnson, Mater. Res. Soc. 16 (2001) 2513–2518.
[17] K. Hajlaoui, A.R. Yavari, B. Doisneau, A. LeMoulec, W.J. Botta, G. Vaughan, A.L. Greer, A. Inoue, W. Zhang, A. Kvick, Scr. Mater. 54 (2006) 1829–1834.
[18] X.F. Ding, J.P. Lin, L.Q. Zhang, H.L. Wang, G.J. Hao, G.L. Chen, J. Alloys. Comp. 506 (2010) 115–119.
[19] Y.B. Wang, M.L. Sui, E. Ma, Philos. Mag. Lett. 87 (2007) 935–942.
[20] J.T.M. De Hosson, Micro Res. Tech. 72 (2009) 250–260.
[21] H. Rösner, N. Boucharat, J. Markmann, K.A. Padmanabhan, G. Wilde, Mater. Sci. Eng. A 525 (2009) 102–106.
[22] Z.W. Shan, J. Li, Y.Q. Cheng, A.M. Minor, S.A.S. Asif, O.L. Warren, E. Ma, Phys. Rev. B 77 (2008) 155419.
[23] P. Murali, R. Narasimhan, T.F. Guo, Y.W. Zhang, H.J. Gao, Scr. Mater. 68 (2013) 567–570.
[24] W.H. Jiang, F.X. Liu, P.K. Liaw, H. Choo, Appl. Phys. Lett. 90 (2007) 81903–81905.
[25] F. Shimizu, S. Ogata, J. Li, Mater Trans. 48 (2007) 2923–2927.
[26] R.T. Ott, F. Sansoz, T. Jiao, D. Warner, C. Fan, J.F. Molomari, K.T. Ramesh, T.C. Hufnagel, Metal. Mater. Trans. A 37 (2006) 2006–3251.
[27] F. Shimizu, S. Ogata, J. Li, Acta Mater. 54 (2006) 4293–4298.
[28] M.D. Demetriou, M.E. Launey, G. Garrett, J.P. Schramm, D.C. Hofmann, W.L. Johnson, R. Ritchie, Nat. Mater. 10 (2011) 123–128.
[29] F. Mompioua, M. Legrosa, T. Radeticb, U. Dahmenb, D.S. Gianolac, K.J. Hemker, Acta Mater. 60 (2012) 2209–2218.
[30] C. Jeon, D.J. Ha, C.P. Kim, S. Lee., Metal. Mater. Trans. A 43A (2012) 3663–3674.
[31] M.Q. Jiang, Z. Ling, J.X. Meng, L.H. Dai, Philos. Mag. 88 (2008) 407–426.
[32] M. Heggen, F. Spaepen, M. Feuerbacher, J. Appl. Phys. 97 (2005) 33506–33514.
[33] Z.T. Wang, J. Pan, Y. Li, C.A. Schuh, Phys. Rev. Lett. 111 (2013) 135504–135508.
[34] J.W. Qiao, T. Zhang, F.Q. Yang, P.K. Liaw, S. Pauly, B.S. Xu, Sci. Rep. 3 (2013) 1–6.
[35] T. Zhang, H.Y. Ye, J.Y. Shi, H.J. Yang, J.W. Qiao, J. Alloy Comp. 583 (2013) 593–597.
[36] J.M. Gere, Mechanics of Materials: Analysis of Stress and Strain, China Machine Press, 2002, p. 479–486.
[37] F.F. Wu, Z.F. Zhang, S.X. Mao, Acta Mater. 57 (2009) 257–266.
[38] C.T. Sun, Z.H. Jin, Fracture Mechanics: Crack Tip Plasticity, Academic Press, 2012, p. 123–169.
[39] Y. Ding, C. Wang, M. Li, W. Wang, Mater. Sci. Eng. B 127 (2006) 62–69.
[40] E. Martin, D. Leguillon, C. Lacroix, Comp. Sci. Tech. 61 (2001) 1671–1679.
[41] G. Chen, J.L. Cheng, C.T. Liu, Intermetallics 28 (2012) 25–33.